

Role of binding energies in A–B and AB– complexes in the kinetics of gas phase electron transfer reactions: $A^- + B = A + B^-$ involving perfluoro compounds: SF₆, C₆F₁₁CF₃, C₆F₆

Swapan Chowdhury and Paul Kebarle

Citation: *J. Chem. Phys.* **85**, 4989 (1986); doi: 10.1063/1.451687

View online: <http://dx.doi.org/10.1063/1.451687>

View Table of Contents: <http://jcp.aip.org/resource/1/JCPSA6/v85/i9>

Published by the American Institute of Physics.

Additional information on J. Chem. Phys.


Journal Homepage: <http://jcp.aip.org/>

Journal Information: http://jcp.aip.org/about/about_the_journal

Top downloads: http://jcp.aip.org/features/most_downloaded

Information for Authors: <http://jcp.aip.org/authors>

ADVERTISEMENT



AIPAdvances

Special Topic Section:
PHYSICS OF CANCER

Why cancer? Why physics? [View Articles Now](#)

Role of binding energies in $A^- \cdot B$ and $A \cdot B^-$ complexes in the kinetics of gas phase electron transfer reactions: $A^- + B = A + B^-$ involving perfluoro compounds: SF_6 , $C_6F_{11}CF_3$, C_6F_6

Swapan Chowdhury and Paul Kebarle

Chemistry Department, University of Alberta, Edmonton, Alberta T6G 2G2, Canada

(Received 12 May 1986; accepted 29 July 1986)

Exothermic gas phase electron transfer reactions: $A^- + B = A + B^-$, where A and B are polyatomic molecules with positive electron affinities, generally proceed at collision rates. However, reactions involving $A = SF_6$ or perfluorocycloalkanes have rates which decrease with the exothermicity of the reaction, becoming very slow at low exothermicity. Earlier work attributed this behavior to the presence of an energy barrier, due to a large geometry change for A^- to A. The reaction coordinate used also involves the bond energies $A^- \cdot B$ and $A \cdot B^-$. These were measured in the present work. It was found that the bond energy in $SF_6^- \cdot B$ is much larger than in $SF_6 \cdot B^-$. This difference increases the energy barrier very significantly and is thus an additional cause for the slow electron transfer. The bond energies for several other complexes like: $Cl^- \cdot B$, $Cl^- \cdot SF_6$, $Cl^- \cdot$ perfluorocycloalkanes, and $Cl^- \cdot C_6F_6$ were measured. These provide insights into the nature of the bonding involved. The work was performed with a pulsed electron high pressure mass spectrometer.

INTRODUCTION

Recently,¹⁻⁴ we reported measurements of the electron affinities of a number of compounds including SF_6 ,¹ perfluoromethylcyclohexane,¹ perfluorobenzene, and substituted perfluorobenzenes.⁴ These were determined from measurements of the gas phase electron transfer equilibria (1).



The work included also determinations of the rate constant k_1 for the forward reaction. The rates k_1 were found²⁻⁴ to be equal or near the collision limit k_c for all exothermic reactions where A and B were substituted nitrobenzenes, quinones, SO_2 , and NO_2 . On the other hand, reactions involving SF_6 and $C_6F_{11}CF_3$ were found to be very slow except when the exothermicity was very high.¹ Very slow electron transfer involving SF_6 had been reported earlier by Fehsenfeld⁵ and Streit and others,⁶ however the investigation from this laboratory¹ was more detailed since it included determinations of the temperature dependence of k_1 and utilized a large number of reactants whose electron affinities had become available through the equilibria (1) determinations.¹⁻⁴

The conclusion reached in the earlier work¹ was that the slow rates involving SF_6 and probably also $C_6F_{11}CF_3$ are due to a large change of geometry occurring on formation of the negative ion. These conclusions were supported by results from theoretical calculations by Hay⁷ which predicted a considerable increase in the S-F distance on formation of SF_6^- . Geometry changes are known to lead to an energy barrier for electron transfer. The reaction coordinate used for the gas phase case (see Fig. 1, Results and Discussion) also contains the binding energies of the adducts $SF_6^- \cdot B$ and $SF_6 \cdot B^-$ where B is the other reactant. Since these binding energies were not available at the time, their magnitude was estimated and the model was found in qualitative agreement with the experimental rates.¹

The present work reports measurements of the relevant binding energies of the adducts. As will be seen, the values obtained are quite different from what was estimated. Furthermore, the specific bonding changes observed turn out to play an important role in the slow electron transfer mechanism.

EXPERIMENTAL

The apparatus and techniques used were the same as those described in the earlier work.^{1,9}

RESULTS AND DISCUSSION

The relevant rate constants k_2 for reaction (2) measured in our earlier work¹ are summarized in Table I. Included in the table are the calculated heights of the internal barriers E^\ddagger ,



and the enthalpy and free energy changes ΔH_2^0 , ΔG_2^0 for reaction (2). The reaction coordinate adopted¹ for reaction (2) is shown in Fig. 1(a). The double minimum potential with the internal barrier E^\ddagger is the standard reaction coordinate^{8,9} used for bimolecular gas phase ion-molecule reactions. At low pressures the collision complex $A^- \cdot B$ is not deactivated by collisions, i.e., there is energy and angular momentum conservation as the collision pair proceeds from reactants to products. It can be shown^{8,9} that the overall forward rate constant k is given by Eq. (3) (for notation see Fig. 1):

$$k = \frac{k_c k_p}{k_p + k_b} \quad (3)$$

When E^\ddagger is small such that the energy gap ΔE_0^\ddagger is negative and its absolute value is large, $k_p \gg k_b$, and the reaction proceeds at collision rates and has the lack of temperature de-

TABLE I. Rate constants k^a and calculated^b energy barriers^c E^\ddagger for reactions $A^- + B = A + B^-$.

	A ^d	B ^d	($-\Delta H^0$) ^e	($-\Delta G^0$) ^e	(E^\ddagger) ^b	($k \times 10^{10}$) ^c
1	SF ₆	3-CF ₃ NB	7.9	2.4	7.4	0.005
2	SF ₆	3-NO ₂ NB	13.9	7.7	5.4	0.6
3	SF ₆	4-CNNB	15.8	9.5	4.8	1
4	SF ₆	4-NO ₂ NB	22.1	15.1	2.9	10
5	SF ₆	F ₄ BQ	38.7	31.7	0.3	14
6	C ₆ F ₁₁ CF ₃	3-CF ₃ NB	7.6	6.2	...	<0.005
7	C ₆ F ₆	2,3-(CH ₃) ₂ NB	...	4.6	...	20
8	C ₆ F ₅ CN	3-FNB	3.2	1.0	...	19

^aSF₆ and C₆F₁₁CF₃ data from Grimsrud (Ref. 1), C₆F₆ and C₆F₅CN from Chowdhury (Ref. 4).

^bD. E. Richardson (Ref. 10), height of internal barrier, see Fig. 1.

^cEnergy in kcal/mol, k in cm³ molecule⁻¹ s⁻¹.

^dNB stands for nitrobenzene and BQ for benzoquinone.

^eEnthalpy and free energy change for reaction: $A^- + B = A + B^-$, values from Kebarle (Refs. 1–4), see particularly Table IV, Ref. 4(b).

pendence observed for these rates. (See B = tetrafluoroquinone Table I.) For larger E^\ddagger where E_0^\ddagger is still negative and its absolute value equal to a few to several kcal/mol, $k_p < k_b$, and the temperature dependence is negative, i.e., k

decreases with increase of temperature (B = 4-NO₂NB and 4-CNNB, see Table I). Finally as ΔE_0^\ddagger approaches zero or becomes positive, $k_p < k_b$, and the temperature dependence becomes positive.^{1,8,9} For electron transfer reactions in the absence of solvent molecules, the barrier E^\ddagger is generally assumed to be due to geometry changes between the neutral and negative ion for A and B. The barriers E^\ddagger given in Table I were calculated by Richardson¹⁰ on the basis of the Marcus equations¹¹ and theoretical geometries of Hay⁷ for SF₆ and SF₆⁻. Richardson assumed essentially minimal geometry changes for B to B⁻. Similar values for E^\ddagger were obtained in the earlier work¹ by a qualitative estimate based on similar geometry change assumptions.

The parabolic potential wells shown in Fig. 1 for SF₆⁻ · B and SF₆ · B⁻ are drawn to scale potential energies for SF₆⁻ and SF₆ for the symmetric S–F stretch, based on Hay's⁷ calculations. The reaction coordinate in this region only is assumed to be the S–F distance. This is in line with the expected minimal geometry change from B to B⁻. The resulting barrier E^\ddagger in the figure thus represents an approximate graphical solution for the Marcus barrier, due to symmetric S–F changes, given in Table I.

In a qualitative discussion of reaction (2), the electron transfer involving the least exothermic reaction (B = 3-CF₃NB) and $E^\ddagger \approx 7.4$ kcal/mol (Table I) is of special interest. For this slowest reaction, k_2 was found to be lower by 10⁴ relative to the collision rate and the Arrhenius plot of k_2 , while not giving a straight line was found to have positive temperature dependence.¹ For this reaction one expects $E^\ddagger > D(\text{SF}_6^- - \text{B})$ and $\Delta E_0^\ddagger > 0$, see Fig. 1(a). The value of the adduct binding energy was not available at the time, however on the basis of a comparison of related binding energies it was concluded that $D(\text{SF}_6^- - \text{B}) \approx 7$ kcal/mol is a possible value, which was consistent with the expected reaction coordinate.

Recently it occurred to us that $D(\text{SF}_6^- - \text{B})$ could be measured experimentally by studying reaction (2) at a low temperature. Since the rate decreases with temperature, for B = CF₃NB, it might be possible to collisionally stabilize the SF₆⁻ · CF₃NB adduct and measure the equilibrium (4). Such an approach had been used successfully in earlier

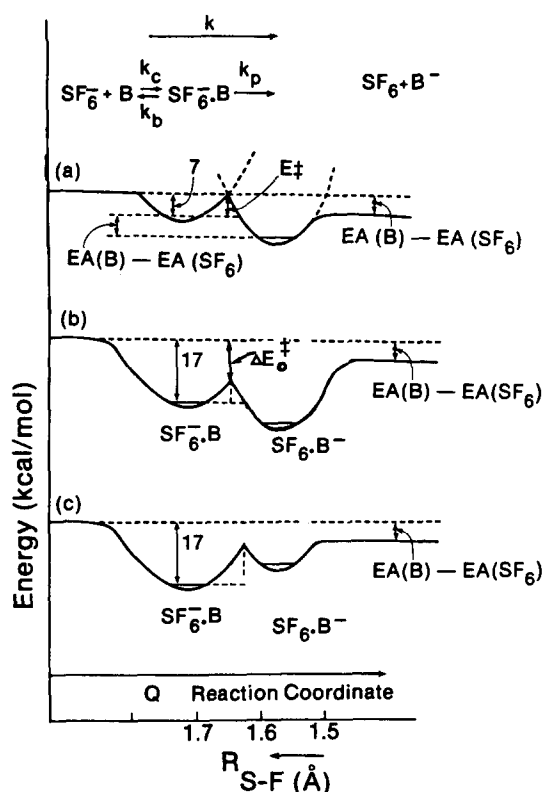


FIG. 1. Reaction coordinate for reaction (2) $\text{SF}_6^- + \text{B} = \text{SF}_6 + \text{B}^-$, where B = 3-CF₃ nitrobenzene. Internal barrier E^\ddagger due to geometry change between SF₆ and SF₆⁻. (a) Reaction coordinate used in earlier work (Ref. 1). Values of bond energies $D(\text{SF}_6^- - \text{B}) \approx D(\text{SF}_6 - \text{B}^-) \approx 7$ kcal/mol were assumed. (b) Reaction coordinate after measurement of $D(\text{SF}_6^- - \text{B}) \approx 17$ kcal/mol and with assumption $D(\text{SF}_6^- - \text{B}) \approx D(\text{SF}_6 - \text{B}^-)$. (c) Reaction coordinate with measured $D(\text{SF}_6^- - \text{B})$. The barrier E^\ddagger is assumed to be only due to geometry changes between SF₆⁻ and SF₆ which consist of a symmetric shortening of the S–F bonds in the region of E^\ddagger , therefore in the region of E^\ddagger , (only) the reaction coordinate is represented by the S–F bond length.

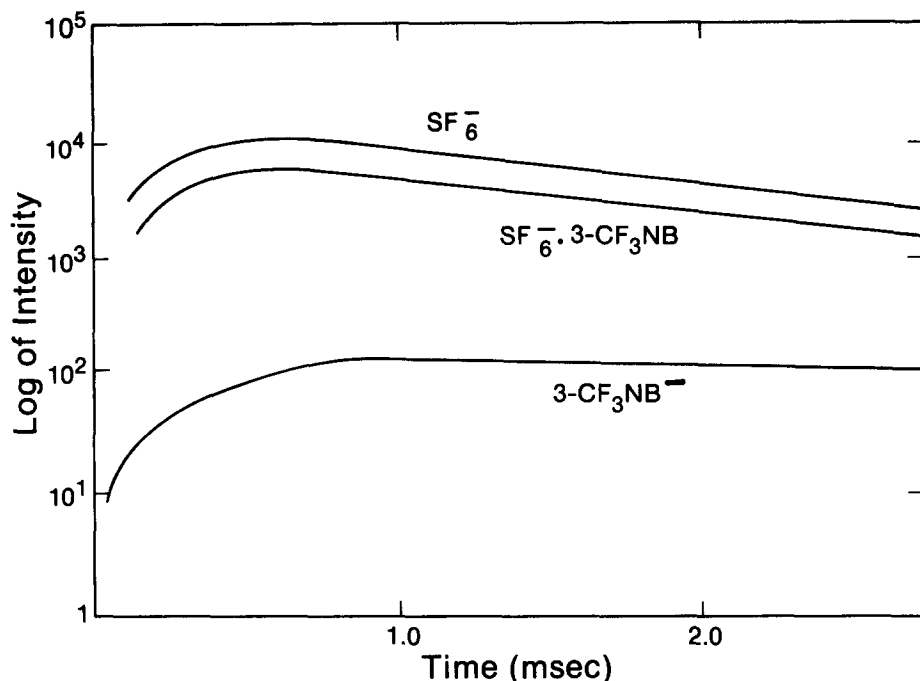


FIG. 2. Observed ion intensities after ionizing electron pulse. Ion source at 69 °C contains: 3 Torr methane as bath gas, 113 mTorr SF_6 , and 3.5 mTorr 3- CF_3 nitrobenzene = B. SF_6^- formed by electron capture engages in adduct forming equilibrium $\text{SF}_6^- + \text{B} = \text{SF}_6^- \cdot \text{B}$. Evidence for this equilibrium is provided by constant distance between logarithmic intensities of the ions. Slow electron transfer to B leads to formation of B^- .

work.⁹ The ion-intensity time dependence of such a lower temperature run is shown in Fig. 2:



Given are the logarithms of the measured ion intensities in function of the time after the short electron pulse. Due to the logarithmic plot, two ions which have an intensity ratio that is constant with time maintain a constant vertical distance from each other. This is the case for SF_6^- and $(\text{SF}_6^- \cdot 3\text{-CF}_3\text{NB})^-$. The $3\text{-CF}_3\text{NB}^-$ ion is seen to have a different time dependence. The constant ion ratio is consistent with the expected equilibrium (4). Both ions engaged in the equilibrium decrease gradually with time mostly due to diffusion to the wall.¹⁻⁵ The electron transfer reaction (2) from SF_6^- to 3- CF_3NB is still occurring, but very slowly, at the low experimental temperature. In the run shown in Fig. 2

the electron transfer rate is close to the diffusion loss of 3- CF_3NB^- and this leads to the observed approximate time invariance of the $3\text{-CF}_3\text{NB}^-$ intensity, observed for $t > 1$ ms.

The dimer ion $(3\text{-CF}_3\text{NB})_2^-$ was also observed in the run used for Fig. 2. This ion, which is not shown in the figure, had similar intensity as the monomer $3\text{-CF}_3\text{NB}^-$ and the ratio of these two ions was constant with t , which means that the monomer and dimer were in equilibrium. A similar run but involving the next slowest reaction (2) where $\text{B} = 3\text{-NO}_2\text{NB}$, see Table I, is shown in Fig. 3. The faster rate of electron transfer is evident. Significantly SF_6^- and $\text{SF}_6^- \cdot 3\text{-NO}_2\text{NB}$ decrease together, i.e., are involved in a fast equilibrium. The products of the electron transfer, $3\text{-NO}_2\text{NB}^-$ and $(3\text{-NO}_2\text{NB})_2^-$, are also in equilibrium. Even though the adduct $3\text{-NO}_2\text{NB}^- \cdot \text{SF}_6$ has the same mass (314) as $\text{SF}_6^- \cdot 3\text{-NO}_2\text{NB}$, significant concentrations of 3-

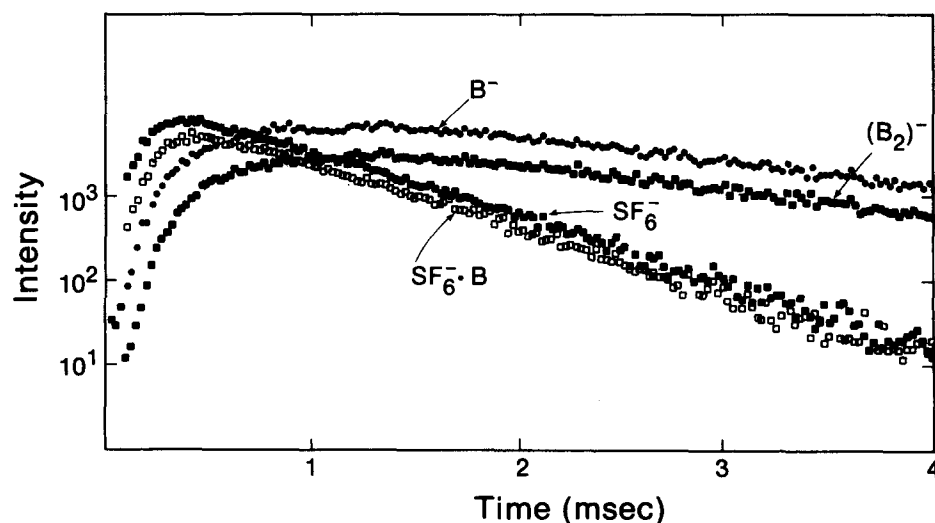


FIG. 3. Ion intensities after ionizing electron pulse. Runs similar to that in Fig. 2 but with $\text{B} = 3\text{-dinitrobenzene (3-NO}_2\text{NB)}$. SF_6^- and $\text{SF}_6^- \cdot \text{B}$ are in equilibrium. B^- and B_2^- are in equilibrium. Electron transfer from SF_6^- and $\text{SF}_6^- \cdot \text{B}$ to B is faster than with $\text{B} = 3\text{-CF}_3\text{NB}$ used in run of Fig. 2 60 °C, methane 3 Torr, SF_6 29 mTorr, B 0.3 mTorr. Actual experimental points shown in Fig. 3 but not in Fig. 2.

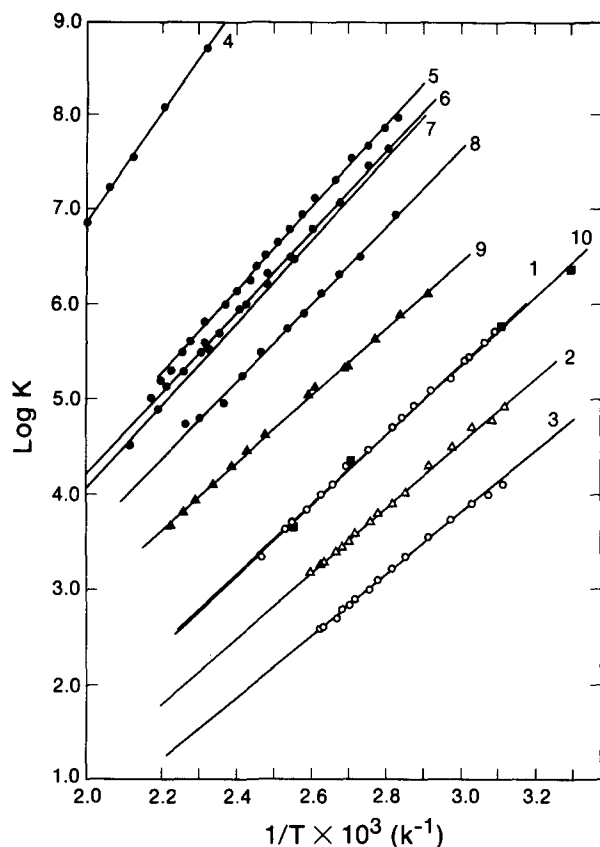


FIG. 4. van't Hoff plots of equilibrium constants K for adduct forming reactions: $A^- + B = A^- \cdot B$. Standard state 1 atm. Numbers correspond to reactions given in Table II.

$\text{NO}_2\text{NB}^- \cdot \text{SF}_6$ are obviously not formed. This follows from the fact that the mass 314 is exactly parallel over the full time range to the SF_6^- ion, i.e., 314 is in exact ion equilibrium with SF_6^- and this means practically all the 314 ion is $\text{SF}_6^- \cdot 3\text{-NO}_2\text{NB}$.

On the basis of a number of runs similar to those illus-

trated in Figs. 2 and 3 and undertaken at different temperatures, equilibrium constants K_4 for the adduct forming reactions (4) leading to $\text{SF}_6^- \cdot \text{B}$ were determined. The van't Hoff plots of the K_4 are shown in Fig. 4 and the resulting ΔG° , ΔH° , and ΔS° data are given in Table II.

The $-\Delta H_4^\circ$ for $\text{B} = 3\text{-CF}_3\text{NB}$ is 18 kcal/mol, which is much larger than the earlier assumed,¹ $-\Delta H_4^\circ \approx 7$ kcal/mol. The new result is incorporated into a new reaction coordinate shown in Fig. 1(b). Evidently, the barrier E^\ddagger of 7.4 kcal/mol is now much too small so that the reaction coordinate in Fig. 1(b) leads to a large $-\Delta E_0^\ddagger$ and is thus inconsistent with the observed very slow kinetics. However the reaction coordinates in Fig. 1(b), as well as in Fig. 1(a), were obtained by making the assumption that the binding energies $D(\text{SF}_6^- \cdot \text{B}) \approx D(\text{SF}_6^- \cdot \text{B}^-)$, an assumption that was justified when both binding energies were unknown. Obviously this equality need not be present since the two adducts are distinct chemical entities that can engage in distinctly different bonding. In fact the failure to observe the adduct $\text{SF}_6^- \cdot \text{B}^-$ in Figs. 2 and 3 is evidence that the bonding in $\text{SF}_6^- \cdot \text{B}^-$ is very much weaker than that for $\text{SF}_6^- \cdot \text{B}$.

An upper limit of the adduct $\text{SF}_6^- \cdot \text{B}^-$ equilibrium constant can be obtained from runs like that shown in Fig. 3. As was discussed above, the fact that the logarithmic intensities of SF_6^- and $(\text{SF}_6^- \cdot \text{B})^-$ are exactly parallel shows that $(\text{SF}_6^- \cdot \text{B})^-$ is predominantly $\text{SF}_6^- \cdot \text{B}$. By estimating the possible deviation from this parallel behavior, at longer reaction times, the maximum possible concentration of $\text{SF}_6^- \cdot \text{B}^-$ can be estimated and the maximum equilibrium constant K for the adduct formation evaluated. The result given as $\Delta G^\circ = -RT \ln K$ is shown in Table II. Assuming $\Delta S^\circ \approx 20.0$ cal/deg a ΔH° can be also estimated. This value, see Table II, is $D(\text{B}^- \cdot \text{SF}_6) < 8$ kcal/mol, which means that $D(\text{SF}_6^- \cdot \text{B}) - D(\text{SF}_6^- \cdot \text{B}^-) > 10$ kcal/mol, which is a very large difference indeed!

Taking this difference into account one can draw a reaction coordinate energy diagram which uses the individual

TABLE II. Binding energies^a in $A^- \cdot B$ from equilibria $A^- + B = A^- \cdot B$.

	A ⁻	B	$-\Delta G^\circ(300\text{ K})$	$-\Delta H^\circ$	$-\Delta S^\circ$
1	SF_6^-	3- CF_3NB	9.0	17.0	26.7
2	SF_6^-	3-FNB	7.9	15.7	26.1
3	SF_6^-	NB	6.7	14.9	27.5
4	Cl^-	F_4BQ	20.2	27.0	22.7
5	Cl^-	4-CN · NB	14.0	20.0	20.0
6	Cl^-	3- CF_3NB	14.1	19.5	17.9
7	Cl^-	$\text{C}_6\text{F}_5\text{CN}$	13.5	19.9	21.2
8	Cl^-	3-FNB	12.3	18.7	21.2
9	Cl^-	NB	10.5	16.3	19.4
10	Cl^-	C_6F_6	8.8	16.8	26.9
11	Cl^-	BQ	9.5
12	Cl^-	C_6H_6	3.8
13	Cl^-	SF_6	≤ 1.8
14	$\text{C}_6\text{F}_{11} \cdot \text{CF}_3^-$	NB	6.7
15	Cl^-	$\text{C}_6\text{F}_{11}\text{CF}_3$	≤ 1.8
16	3- $\text{NO}_2 \cdot \text{NB}^-$	SF_6	$< 1.7(333\text{ K})$	$< 8.4^b$...
17	4- NO_2NB^-	SF_6	≤ 1.9	$\leq 8.5^b$...

^a All energies in kcal/mol, entropy in cal/deg, standard state 1 atm, NB stands for nitrobenzene, BQ for benzoquinone.

^b ΔS°_{16} , assumed to be -20 cal/deg.

adduct binding energies. This diagram is shown in Fig. 1(c), where the assumption has been made that $D(\text{SF}_6\text{--B}^-)$ is the same for $\text{B} = 3\text{-CF}_3\text{NB}$ and $3\text{-NO}_2\text{NB}$. Actually, because of increased charge delocalization in $3\text{-NO}_2\text{NB}^-$ one expects $D(\text{SF}_6\text{--}3\text{-NO}_2\text{NB}^-)$ to be slightly smaller.

The accurate accounting of the adduct binding energies in the reaction coordinate Fig. 1(c), changes the picture completely. The electron transfer reaction based on the zero point levels of the two complexes has now become endothermic rather than exothermic and the internal barrier E^\ddagger due to SF_6 geometry change is thereby raised such that $-\Delta E_0^\ddagger$ is quite small again. Furthermore, since there is a change in the adduct geometries, this change must also become part of the reaction coordinate, an effect not taken into account in the evaluation of E^\ddagger (Table I and Fig. 1) which considers only S-F bond length changes. Consideration of the adduct changes will lead to a further increase of the internal barrier E^\ddagger so that $E^\ddagger \approx D(\text{SF}_6\text{--B})$ becomes possible and the kinetic model becomes again compatible with the observed kinetics.

It is of considerable interest to enquire into the reasons for the large difference in the bond energies $D(\text{SF}_6\text{--B})$ and $D(\text{SF}_6\text{--B}^-)$. A more general examination of the bonding involved will be of importance also for other $(\text{A} \cdot \text{B})^-$ systems.

The temperature dependence of adduct forming equilibria for several systems including reaction (5) was measured. The van't Hoff plots are shown in Fig. 4 and the corresponding thermochemical data in Table II. Earlier results^{3,12} for the equilibria (5) and (6) indicated that the complexes formed:



essentially hydrogen bonded structures. Thus when $\text{B} =$ nitro benzenes, the electron withdrawing substituents on the benzene induce partial positive charges on the aromatic hydrogens and the resulting most positive hydrogens engage in hydrogen bonding to the negative ion. The occurrence of this type of bonding was supported by results from STO-3G theoretical calculations.¹² The type of bonding proposed is illustrated in Fig. 5(a) which gives the bonding in $\text{SF}_6 \cdot 3\text{-CF}_3\text{NB}$. The hydrogen involved may be that shown in the figure or the hydrogen which is in position 3 to both

the NO_2 and CF_3 substituents.³ The similarity between the bonding observed in $\text{SF}_6^- \cdot \text{B}$, $\text{Cl}^- \cdot \text{B}$, and $\text{NO}_2^- \cdot \text{B}$ is evident when one examines the order of bond energies for the three anions. Thus in Table II, $D(\text{SF}_6^- \cdot \text{B})$ decreases in the order $\text{B} = 3\text{-CF}_3\text{NB}$; 3-FNB ; NB , the same order being observed for $D(\text{Cl}^- \cdot \text{B})$ see Table II and NO_2^- see Ref. 3. The order is dictated by the decreasing electron withdrawing power of the substituents on the benzene ring.^{3,12} The weakest $\text{Cl}^- \cdot \text{B}$ bond is found for $\text{B} =$ benzene, see Table II, where electron withdrawing substituents are completely absent. The binding energies $\text{SF}_6^- \cdot \text{B}$ are smaller than those for $\text{Cl}^- \cdot \text{B}$, a result that could have been anticipated from the larger size of SF_6^- relative to Cl^- . However the difference is not as large as might have been expected.¹ The relatively strong bonding in $\text{SF}_6^- \cdot \text{B}$ should be due to the high electronegativity of the fluorine atoms. Thus, the rather small F, involved in the hydrogen bond shown in Fig. 5(a), probably has a relatively large net negative charge and this makes it a very suitable hydrogen acceptor.

On the other hand, everything is unfavorable to bonding in $\text{B}^- \cdot \text{SF}_6$ and $\text{Cl}^- \cdot \text{SF}_6$. The adducts $\text{B}^- \cdot \text{SF}_6$ were not detected in the present work, see Table II. SF_6 is not suitable because it has the wrong charge distribution. Thus, the $\text{S}^+ \text{--} \text{F}^-$ bond dipoles in SF_6 result in a dodecapole with negative charge on the outside of the molecule which shields the SF_6 from interaction with negative centers in B^- , see Fig. 5(b), or Cl^- .

The geometry changes occurring on formation of the negative ion $\text{C}_6\text{F}_{11}\text{CF}_3^-$ from the neutral are not known, however the very low rate constant for electron transfer from $\text{C}_6\text{F}_{11}\text{CF}_3^-$ to B , see Ref. 1 and Table I reaction 8, is probably primarily due to such a geometry change, i.e., the situation in this respect is probably similar than that for SF_6 and SF_6^- . Another similarity is also present in the bonding energy changes of the adducts. Thus $\text{C}_6\text{F}_{11}\text{CF}_3^-$ bonds to NB and probably also to CF_3NB about equally well as SF_6^- , compare data for adduct reactions 3 and 14 in Table II. Similarly, negative ions bond very poorly to $\text{C}_6\text{F}_{11}\text{CF}_3$ as was the case for SF_6 , compare reactions 13 and 15, Table II. Thus it appears that the reasons for the slow electron transfer from $\text{C}_6\text{F}_{11}\text{CF}_3^-$ are the same as those for SF_6^- . Low rate constants were observed also for perfluorocyclohexane¹ and it is likely that the factors involved for this compound and other perfluorocycloalkanes will be similar to those for SF_6 and $\text{C}_6\text{F}_{11}\text{CF}_3$.

Electron transfer reactions involving perfluorobenzene were studied also.⁴ Exothermic electron transfer from C_6F_6^- was found to be near the collision limit, see reaction 7, Table I. While some geometry change is expected between C_6F_6 and C_6F_6^- , see Chowdhury⁴ and references therein, these changes could be relatively small so that they do not lead to a large barrier E^\ddagger . Considering the weak bonding observed for $\text{B}^- \cdot \text{SF}_6$ and $\text{B}^- \cdot \text{C}_6\text{F}_{11}\text{CF}_3$, one might have expected that $\text{B}^- \cdot \text{C}_6\text{F}_6$ would be also weakly bonded. Results for the bonding in $\text{Cl}^- \cdot \text{C}_6\text{F}_6$ are given in Table II. Surprisingly C_6F_6 bonds quite strongly in spite of the fact that it does not have periodic hydrogens. Since the π clouds represent regions of negative charge C_6F_6 is also not suitable for electrostatic bonding where the Cl^- approaches the ben-

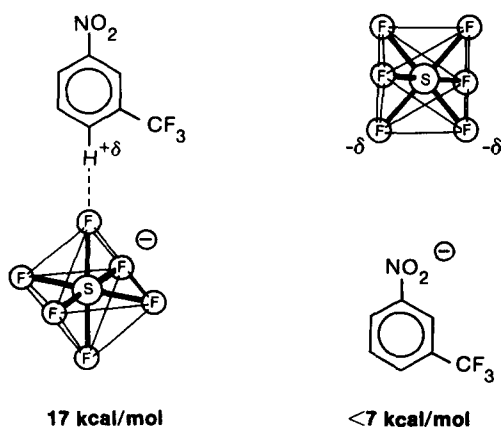


FIG. 5. Bonding in $\text{SF}_6^- \cdot \text{B}$ and $\text{B}^- \cdot \text{SF}_6$ where $\text{B} = 3\text{-CF}_3\text{NB}$.

zene ring along the symmetry axis, see French¹² and Sunner.¹³ The reasons for strong bonding observed in $\text{Cl}^- \cdot \text{C}_6\text{F}_6$ are not yet clear. A "chemical" type of bond, i.e., a $\pi^* \text{Cl}^- \text{C}_6\text{F}_6$ charge transfer complex is one possibility that could be considered. Additional bond energy measurements between negative ions and C_6F_6 and other related systems are underway in this laboratory. These might provide insights into the nature of the bonding involved. In any case, the relatively strong bonding of negative ions to C_6F_6 removes excessive adverse bonding changes from $\text{C}_6\text{F}_6^- \cdot \text{B}$ to $\text{B}^- \cdot \text{C}_6\text{F}_6$, as a factor leading to slow electron transfer from C_6F_6^- and this is in agreement with the observed fast electron transfer kinetics for C_6F_6^- .

ACKNOWLEDGMENT

This work was supported by the Canadian Natural Sciences and Engineering Research Council.

- ¹E. P. Grimsrud, S. Chowdhury, and P. Kebarle, *J. Chem. Phys.* **83**, 1059 (1985).
- ²E. P. Grimsrud, G. Caldwell, S. Chowdhury, and P. Kebarle, *J. Am. Chem. Soc.* **107**, 4627 (1985).
- ³E. P. Grimsrud, S. Chowdhury, and P. Kebarle, *Int. J. Mass Spectro. Ion Processes* **68**, 57 (1986).
- ⁴(a) S. Chowdhury, E. P. Grimsrud, T. Heinis, and P. Kebarle, *J. Am. Chem. Soc.* **108**, (3630) (1986); (b) *J. Phys. Chem.* **90**, 2747 (1986).
- ⁵F. C. Fehsenfeld, *J. Chem. Phys.* **54**, 438 (1971).
- ⁶G. E. Streit, *J. Chem. Phys.* **77**, 826 (1982), and references therein.
- ⁷P. J. Hay, *J. Chem. Phys.* **76**, 502 (1982).
- ⁸W. N. Olmstead and J. I. Brauman, *J. Am. Chem. Soc.* **99**, 4219 (1977); W. E. Farneth and J. I. Brauman, *ibid.* **98**, 7891 (1976).
- ⁹K. Hiraoka and P. Kebarle, *J. Chem. Phys.* **63**, 394 (1975); *J. Am. Chem. Soc.* **98**, 6119 (1976); D. K. Sen Sharma and P. Kebarle, *ibid.* **104**, 19 (1982); G. Caldwell, T. F. Magnera, and P. Kebarle, *ibid.* **106**, 959 (1984).
- ¹⁰D. E. Richardson, *J. Phys. Chem.* **90**, 3697 (1986).
- ¹¹N. Sutin, *Prog. Inorg. Chem.* **30**, 441 (1983).
- ¹²M. W. French, S. Ikuta, and P. Kebarle, *Can. J. Chem.* **60**, 1907 (1982).
- ¹³J. Sunner, K. Nishizawa, and P. Kebarle, *J. Phys. Chem.* **85**, 1814 (1981).